Soft Comput (2015) 19:459–470
DOI 10.1007/s00500-014-1264-2

METHODOLOGIES AND APPLICATION

Intuitionistic fuzzy *c*-means clustering algorithm with neighborhood attraction in segmenting medical image

Ching-Wen Huang · Kuo-Ping Lin · Ming-Chang Wu · Kuo-Chen Hung · Gia-Shie Liu · Chih-Hung Jen

Published online: 27 March 2014

Abstract Fuzzy segmentation methods, especially fuzzy *c*-means algorithms, have been widely used in medical imaging in past decades. This paper proposes a novel neighborhood intuitionistic fuzzy *c*-means clustering algorithm with a genetic algorithm (NIFCMGA). This new clustering algorithm technology can retain the advantages of an intuitionistic fuzzy *c*-means clustering algorithm to maximize benefits and reduce noise/outlier influences through neighborhood membership. Furthermore, the genetic algorithms were used simultaneously to select the optimal parameters of the proposed clustering algorithm. This proposed technology has been successfully applied to the clustering of different regions of magnetic resonance imaging and computerized tomography scanning, which may be extended to the diagnosis of abnormalities. Comparisons with other approaches demonstrate the superior performance of the proposed NIFCMGA.

Keywords Fuzzy segmentation · Fuzzy *c*-means · Medical images · Neighborhood intuitionistic fuzzy *c*-means clustering algorithm

Communicated by T.-P. Hong.

C.-W. Huang
Department of Diagnostic Radiology, Shin Kong Wu Ho-Su Memorial Hospital, Shihlin, Taipei 111, Taiwan

K.-P. Lin (✉) · M.-C. Wu · G.-S. Liu · C.-H. Jen
Department of Information Management, Lunghwa University of Science and Technology, Taoyuan 333, Taiwan
e-mail: kplin@mail.lhu.edu.tw

K.-C. Hung
Department of Computer Science and Information Management, Hungkuang University, Taichung 433, Taiwan

1 Introduction

Segmentation is a process of partitioning an image space into several non-overlapping meaningful homogeneous regions. Segmentation is a crucial step toward image analysis because it can be stated in terms of partitioning the image into different regions, each having homogeneous features. In general, segmentation imaging adopts a clustering (unsupervised) method. Notably, clustering technology has been widely applied to problem solving, decision-making applications, and image segmentation. During recent years, imaging has widely required fuzzy technology because of the uncertainty present in terms of vagueness of class definitions, boundaries, and imprecise gray levels. In recent years, imaging has required the use of fuzzy technology to compensate for the uncertainty associated with class definitions, boundaries, and imprecise gray levels. For example, the imprecision of values at various pixels can result in ambiguity, while membership value gradations can reduce the degree to which boundary regions are defined. The value of fuzzy techniques is their ability to incorporate the ambiguities in the performance of image processing tasks.

Among the various clustering techniques, the most widely used techniques include the hard c-means (k-means), fuzzy c-means (FCM), their variants, evolutionary algorithms, and artificial neural networks (Bezdek 1981; de Jesús Rubio and Pacheco 2009; Hruschka et al. 2009; Jain and Dubes 1988; Hwang and Rhee 2007; Srivastava et al. 2012; Yang 1993; Zhang 2000). Furthermore, among fuzzy clustering technologies, fuzzy c-means (FCM) is the most important for image segmentation (Bezdek et al. 1993). FCM assigns each pixel to fuzzy clusters without labels and allows pixels to belong to multiple clusters with varying degrees of membership. Much research has applied FCM to image segmentation, especially medical images, because medical images always

include considerable uncertainty and unknown noise. Clark et al. (1994) used FCM for segmenting and labeling MRI volumes of the brain. Their study combines knowledge-based techniques where unsupervised fuzzy clustering could effectively segment and label normal MRI slices of the brain. Tolias and Panas (1998) proposed a fuzzy vessel tracking algorithm for retinal images. The pre-process of fuzzy vessel tracking algorithms adopted FCM to define the membership function of linguistic values and then used a tracking algorithm to modify the membership function. Their proposed algorithm resulted in good tracking of well-defined vessels in the image and missed only vessels of small diameter and low contrast. Pham and Prince (1999) proposed an adaptive fuzzy c-means algorithm (AFCM) for the fuzzy segmentation of magnetic resonance brain images. The AFCM can obtain lower error rates than FCM. Shen et al. (2005) used neighborhood attraction to extend the FCM clustering algorithm to MRI fuzzy segmentation. Moreover, the parameters of FCM can be optimized using a neural network model. Maji and Pal (2008) proposed rough-fuzzy c-means (RFCM) for brain MRI segmentation. The rough set mechanism can assist FCM to handle overlapping classes. Hence, the RFCM can achieve better performance in brain MRI segmentation cases. He et al. (2008) proposed an integrated approach for the segmentation of multi-spectral MRI. This proposed method takes into account the non-spherical occupancy and volume differences in the clusters in the feature space. Qualitative and quantitative evaluation indicates satisfactory performance of the approach. Kannan et al. (2010) developed an effective robust fuzzy c-means based kernel function for a segmentation of breast and brain MRI. To overcome heavy noise, outliers, and other imaging artifacts, their proposed method develops a novel objective function based on the objective function of FCM that incorporates the robust kernel-induced distance. In experiment results, the proposed method obtains superior clustering results. Chen et al. (2011) developed a generalized multiple-kernel FCM for the image segmentation problem. Simulations of the segmentation of synthetic and medical images demonstrate the flexibility and advantages of the proposed approach. Ji et al. (2011) adopted a novel adaptive method to compute the weights of local spatial factors in the objective function to impose sufficient local spatial continuity. Their proposed modified possibilistic FCM successfully applies to real MRI scenarios. Experimental results show that the proposed method is effective and more robust for various levels of noise and with higher accuracy in the context of brain MRI segmentation. Chaira (2011) proposed an intuitionistic FCM (IFCM) clustering algorithm for medical images. The intuitionistic fuzzy sets (IFSs) consider another uncertainty parameter, which is the hesitation degree that arises while defining the membership function, and thus the cluster centers may converge in a more desirable location than the cluster centers obtained using FCM. Experimental results elicit better performance than conventional FCM and type-2 fuzzy algorithms.

From past research, some phenomena can be observed: (1) the FCM-based clustering algorithm can be successfully applied to medical image segmentation; (2) the defining methods of the membership function will influence the performance of FCM-based clustering algorithms; (3) the FCM-based clustering algorithm should overcome noise/outlier effects when applied to the image segmentation problem. Based on these viewpoints, this study proposes a novel neighborhood intuitionistic fuzzy c-means clustering algorithm. The novel algorithm adopts the advanced concept of intuitionistic fuzzy c-means clustering and, to overcome noise/outliers effects, the objective function and procedure of updating membership consider neighboring pixels.

The remainder of this paper is organized as follows: Sects. 2 and 3 introduce the intuitionistic fuzzy sets and FCM clustering technology, respectively, and Sect. 4 presents the proposed neighborhood intuitionistic fuzzy $c-$means clustering algorithm. Section 5 provides the experimental results of NIFCM in the context of medical imaging; Sect. 6 offers conclusions and suggestions for further research. Table 1 shows the main notations in this paper.

2 Intuitionistic fuzzy sets (IFSs)

Fuzzy set theory, proposed by Zadeh (1965), has been successfully applied in various fields. This theory states that the membership of an element to a fuzzy set is a single value between zero and one. However, in reality, it is not always certain that the degree of non-membership of an element to a fuzzy set is simply equal to 1 minus the degree of membership; i.e., there may be some *hesitation* degree (see definition below). Thus, as a generalization of fuzzy sets, the concept of IFSs was introduced by Atanassov (1986). Bustince and Burillo (1996) showed that this notion coincides with the notion of vague sets (VSs).

The IFSs is put forth as an extension of fuzzy sets. An IFSs A in a fixed set E is an objective with regard to the expression:

$$A = \{\langle x, \mu_A(x), \nu_A(x)\rangle \,|x \in E\} \tag{1}$$

where the functions $\mu_A : E \to [0, 1]$ and $\nu_A : E \to [0, 1]$ denote the degree of membership and the degree of non-membership of the element $x \in E$, respectively. For every $x \in E$:

$$0 \leq \mu_A(x) + \nu_A(x) \leq 1. \tag{2}$$

When $\mu_A(x) + \nu_A(x) = 1$, for every $x \in E$, then the IFSs will degenerate into a fuzzy set. Hence, we can consider a

Table 1 Main notations list

μ	Degree of membership	c	Number of clusters
ν	Degree of non-membership	m	Parameters in updating the clustering membership functions
π	Hesitation degree	α	Yager's intuitionistic fuzzy parameter
d	Distance between data point and center of the cluster	L	number of epochs
θ	Center of the cluster	δ	Tolerance for the solution accuracy
$N\mu$	Modified membership of pixel by neighborhood pixel tuning	E	Error function/fitness function

fuzzy set with its membership function $\mu_A(x)$, having the IFSs expression as:

$$A = \{\langle x, \mu_A(x), 1 - \mu_A(x)\rangle \,|x \in E\}. \tag{3}$$

For each IFSs A in E, the hesitation degree has consideration. We define the hesitation degree of an element $x \in E$ in A by the following expression:

$$\pi_A(x) = 1 - \mu_A(x) - \nu_A(x), \tag{4}$$

we can consider a as a hesitancy degree of x to A. From Eq. (4), it is evident that

$$0 \le \pi_A(x) \le 1 \quad \text{for all } x \in E. \tag{5}$$

Therefore, to describe an intuitionistic fuzzy set completely, we need at least two functions from the triplet, according to Atanassov (1989, 1999): (1) membership function; (2) non-membership function; and (3) hesitation degree.

With regard to intuitionistic fuzzy sets, intuitionistic fuzzy generators or fuzzy complements were created from Yager generating functions (Bustince and Burillo 1996). The fuzzy complement functional is defined as:

$$N(\mu(x)) = g^{-1}(g(1) - g(\mu(x))) \tag{6}$$

where $g(.)$ is an increasing function and g:[0,1]→[0,1].

The Yager class can be generated using the following function in the above Eq. (6):

$$g(x) = x^{\alpha}. \tag{7}$$

So, Yager's intuitionistic fuzzy complement is written as:

$$N(x) = (1 - x^{\alpha})^{1/\alpha}, \alpha > 0 \quad \text{where } N(1) = 0, N(0) = 1. \tag{8}$$

Non-membership values are calculated from Yager's intuitionistic fuzzy complement $N(x)$. Thus, with the help of Yager's intuitionistic fuzzy complement, IFSs become:

$$A = \left\{\left\langle x, \mu_A(x), (1 - \mu_A(x)^{\alpha})^{1/\alpha}\right\rangle | x \in E\right\}. \tag{9}$$

The hesitation degree is:

$$\pi_A(x) = 1 - \mu_A(x) - (1 - \mu_A(x)^{\alpha})^{1/\alpha}. \tag{10}$$

3 Fuzzy c-means algorithm

Clustering analysis involves the discovery of a data structure and partitions a data set into a number of subsets with correlated data. Clustering has been widely applied in several fields, such as taxonomy, geology, business, engineering systems, medicine, and image processing (for example, Bezdek 1981; Yang 1993; Honda and Ichihashi 2004; Kohonen 1997; and Liu and Wang 2007). Among the various partitioning techniques, the most widely used techniques include the hard c-means (k-means), FCM, their variants, and artificial neural networks (for example, Bezdek 1981; Jain and Dubes 1988; Hwang and Rhee 2007; Yang 1993; and Zhang 2000). In FCM and fuzzy clustering concepts, the membership function of clusters can be defined by a distance function; thus, the degrees of memberships may express the proximity of the data to the multi-cluster centers. First, parameters as the number of classify (c), parameter in updating the clustering membership functions (m), number of epochs to carry out (L), and tolerance for the solution accuracy (δ) are set. Subsequently, by the FCM, the initial memberships of the data $x_i, i = 1, \ldots, N$, with the crisp input–output to the clusters j ($j = 1, \ldots, c$) are generated randomly and denoted as $U(l) = [\mu_{ij}^{(l)}]_{N\times c}(l = 0)$ under $\sum_{\forall j} \mu_{ij}^{(l)} = 1 \forall i$. Alternatively, a conventional clustering method may be used, in which a crisp partition of (x_i, y_i)'s to c-clusters can be performed. The procedure of the FCM can be performed with the initial l value set to 0. The FCM objective function can be formulated as follows:

$$J_m(\mu; X) = \sum_{j=1}^{c}\sum_{i=1}^{N}\left(\mu_{ij}^{(l)}\right)^m \times d_{ij}(\boldsymbol{x}_i, \boldsymbol{\theta}_j^{(l)}) \tag{11}$$

where d is the square Euclidean distance between data x_i and center of the cluster j, θ_j. The parameter m is a weighting exponent on each fuzzy membership and determines the amount of fuzziness of the resulting classification. For

$m = 1$, the objective function Eq. (11) reduces to the classical within-group sum of the squared errors objective function and FCM becomes equivalent to the hard clustering technologies. In past research, the commonly set value is $m = 2$ (Pedrycz and Rai 2008; Fan et al. 2009; Chaira 2011).

$$d_{ij}(\boldsymbol{x}_i, \boldsymbol{\theta}_j^{(l)}) = (\boldsymbol{x}_i - \boldsymbol{\theta}_j^{(l)})^T I (\boldsymbol{x}_i - \boldsymbol{\theta}_j^{(l)})$$

$$\mu_{ij}^{(l)} \in [0, 1], \sum_{j=1}^{c} \mu_{ij}^{(l)} = 1, \text{ and } 0 < \sum_{i=1}^{N} \mu_{ij}^{(l)} < N. \tag{12}$$

$$\mu_{ij}^{(l+1)} = \begin{cases} \left(\sum_{h=1}^{c} \left(\frac{d(\boldsymbol{x}_i, \boldsymbol{\theta}_j^{(l+1)})}{d(\boldsymbol{x}_i, \boldsymbol{\theta}_h^{(l+1)})} \right)^{(2/(m-1))} \right)^{-1}, & \text{if } d(\boldsymbol{x}_i, \boldsymbol{\theta}_j^{(l+1)}) > 0, \\ 1, & \text{if } d(\boldsymbol{x}_i, \boldsymbol{\theta}_j^{(l+1)}) = 0, \end{cases}$$

$$\boldsymbol{\theta}_j^{(l+1)} = \frac{\sum_{i=1}^{N} \mu_{ij}^{(l+1)} \boldsymbol{x}_i}{\sum_{i=1}^{N} \mu_{ij}^{(l+1)}}. \tag{13}$$

FCM optimizes the objective function by continuously updating the membership functions and centers of clusters until optimization between iterations is less than a threshold (δ).

4 Neighborhood intuitionistic fuzzy *c*-means algorithm

A new algorithm is proposed here to improve the IFCM method and is applied to a medical imaging system for assisting diagnostic physicians. First, the medical images are uploaded to an images database. Second, the medical images are transformed to a gray matrix, and then the user is able to define the number of clusters. Third, the NIFCM obtains each cluster of pixels. Finally, the original image is colored by a cluster of pixels, allowing a physician to perform their diagnostic duties. The main mechanisms are described in the following section.

$$\mu_{ij}^{(l+1)*} = \begin{cases} 1 - \left(1 - \left(\left(\sum_{h=1}^{c} \left(\frac{d(\boldsymbol{x}_i, \boldsymbol{\theta}_j^{(l+1)})}{d(\boldsymbol{x}_i, \boldsymbol{\theta}_h^{(l+1)})} \right)^{(2/(m-1))} \right)^{-1} \right)^{\alpha} \right)^{1/\alpha}, & \text{if } d(\boldsymbol{x}_i, \boldsymbol{\theta}_j^{(l+1)}) > 0, \\ 1, & \text{if } d(\boldsymbol{x}_i, \boldsymbol{\theta}_j^{(l+1)}) = 0, \end{cases}$$

$$\boldsymbol{\theta}_j^{(l+1)*} = \frac{\sum_{i=1}^{N} \mu_{ij}^{(l+1)*} \boldsymbol{x}_i}{\sum_{i=1}^{N} \mu_{ij}^{(l+1)*}}. \tag{14}$$

4.1 Neighborhood intuitionistic fuzzy *c*-means algorithm

The main construct of NIFCM is based on IFCM (Chaira 2011). To improve upon the FCM method, the construct of IFCM modifies the objective function of the conventional FCM using IFSs and adopts intuitionistic fuzzy entropy (IFE). The IFE is introduced in the clustering (Chaira 2011; Zadeh 1965) that aims in maximizing the good points in the class, and the goal is to minimize the entropy of the histogram of an image in the objective function of NIFCM. Moreover, the membership value of IFCM determines the clustering result, and the membership value of IFCM is determined by the similarity measurement, as in Eq. (12). The similarity measurement is a measure of the difference between the intensity of a pixel and the cluster and has no effective resistance to noise. Therefore, our proposed method considers membership of neighborhoods and the self to modify the membership value of IFCM. This neighborhood attraction can effectively correct the membership of pixel and reduce noise pixel in image processing.

Our proposed NIFCM also retains the advantaged construct of IFCM. The objective function of NIFCM that contains two terms is minimized and is as follows:

$$J_m(NU, v; X) = \sum_{j=1}^{c} \sum_{i=1}^{N} \left(N\mu_{ij}^{(l)} \right)^m \times d_{ij} \left(\boldsymbol{x}_i, \boldsymbol{\theta}_j^{(l)*} \right) + \sum_{j=1}^{c} \pi_j^* e^{1-\pi_j^*}$$

where $N\mu_{ij}$ is modified membership of pixel by neighborhood pixel tuning. $\pi_j^* = \frac{1}{N} \sum_{i=1}^{n} \pi_{ji}, i \in [1, N]$. π_{ji} is the hesitation degree of the ith element in cluster j which can be seen in Eq. (10).

Minimization of J_m is based on suitable tuning $N\mu_{ij}$ (membership matrix) and θ (cluster center) using an iterative process. First, to incorporate intuitionistic fuzzy properties into conventional fuzzy clustering algorithms, the intuitionistic fuzzy membership (μ_{ij}^*), which considers the hesitation degree [Eq. (10)], and cluster center ($\boldsymbol{\theta}_j^*$) values, should be determined through the following equations:

Based on Eq. (14), the tuning membership ($N\mu_{ij}$) can be determined as follows:

$$N\mu_{ij}^{(l+1)} = \mu_{ij}^{(l+1)*} / \left(\mu_{ij}^{(l+1)*} + \sum_{k \in S} \mu_{jk}^{(l+1)*} \right), \tag{15}$$

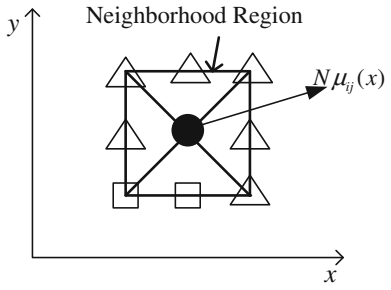

Fig. 1 Neighborhood structure definitions

Table 2 Neighborhood intuitionistic fuzzy c-means algorithm

NIFCM algorithm
Input: data x_i, c, m, intuitionistic fuzzy α
Output: fuzzy partition $N\mu_{ij}$, prototypes θ
Algorithm:
Initial U to random fuzzy partition
Do
Update θ, U according to Eq. (14)
Update $N\mu_{ij}$ according to Eq. (15)
Until termination criteria are satisfied or maximum iterations have been reached Return $N\mu_{ij}$ and θ

where S is neighborhood pixels. The illustration of neighborhood is depicted in Fig. 1. With different numbers of S, the performance of clustering results will be affected. The larger S may easily result in an overfitting phenomenon, in which the image cannot clearly be recognized by a professional physician. Therefore, the number of neighborhood pixels (S) can set 4 or 8 pixels with different images.

The procedure of NIFCM can be stated as follows or Table 2:

Step 1: Determine the number of clusters (c), the parameters in updating the clustering membership functions (m), Yager's intuitionistic fuzzy parameter (α), number of epochs to carry out (L), and the tolerance for the solution accuracy (δ).

Step 2: The initial memberships of the data (x_i, y_i), $i = 1, \ldots, N$, with crisp input–output to the clusters j ($j = 1, \ldots, c$) generated randomly and denoted as $U(l) = [\mu_{ij}^{(l)}]_{N\times c}$ ($l = 0$) under $\sum_{\forall j} \mu_{ij}^{(l)} = 1 \forall i$.

Step 3: Calculate the intuitionistic cluster center (θ_j^*).

Step 4: Update intuitionistic fuzzy membership (μ_{ij}^*).

Step 5: Calculate membership ($N\mu_{ij}$) with neighborhood pixel tuning and the objective function of NIFCM (J_m).

Step 6: If the number of epochs equals a given scale (L) or the tolerance for the solution accuracy equals a given scale (δ), present the optimal membership ($N\mu_{ij}$) is a solution; otherwise, $l = l+1$, and revert to Step 3.

Furthermore, in this study, an error index (E) is used to measure the performance (Yasnoff et al. 1977).

$$E = \frac{|B_{\mathrm{ET}} \cap B_{\mathrm{GT}}| + |F_{\mathrm{ET}} \cap F_{\mathrm{GT}}|}{B_{\mathrm{GT}} + F_{\mathrm{GT}}} \tag{16}$$

where F_{GT} and B_{GT} are the foreground and background area pixels of the ground truth image. F_{ET} and B_{ET} are the foreground and background area pixels of the experimental threshold image.

Parameter selection is also crucial to the success of the NIFCM model, such that suitable parameters for the intuitionistic fuzzy method can noticeably improve performance. Many studies have adopted GAs for the selection of parameters, the results of which have demonstrated the efficacy of this approach (Chang et al. 2009; Jangjit 2009; Tao and Wang 2007). Thus, this study employed a GA (Holland 1975) for the selection of parameters (S, m, and α) in the NIFCM model. GA is evolution-based algorithm, which begins from a population of randomly generated individuals and proceed through generations. In each generation, the fitness of every individual in the population is evaluated. Multiple individuals are then stochastically selected from the current population (according to their fitness), whereupon a new population is formed through crossover and mutation mechanisms. The new population is then used in following iterations of the algorithm until the stop conditions have been satisfied. The operations of GA in the NIFCM with GA (NIFCMGA) model are described as follows:

Step 1 (Initialization): An initial population of chromosomes was randomly generated. The parameters were encoded in a binary format, represented by a chromosome.

Step 2 (Evaluating fitness): In this study, a negative E was adopted as the fitness function.

Step 3 (Selection): According to the fitness function, chromosomes with higher fitness values were more likely to yield offspring in the following generation. Roulette wheel selection was applied for the selection of chromosomes, in which only elite chromosomes were reserved for reproduction.

Step 4 (Crossover and mutation): Mutations were performed randomly by converting a 1 bit into a 0 bit or a 0 bit into a 1 bit. We employed the single-point-crossover principle. Segments of paired chromosomes between two determined break-points were swapped. The rates of crossover and mutation were probabilistically determined.

Step 5 (Next generation): A population for the next generation is assembled.

Step 6 (Stop conditions): If the number of generations equaled a given value, then present the optimal chromosomes as a solution; otherwise, revert to Step 2.

To reduce forecasting errors, the error function (E) was used as a fitness function of the GA. Thus, each iteration

obtained a lower E value. The parameter search procedure was repeated until the stop criterion was reached.

5 Experimental results and discussions

Various imaging modalities, such as MRI, CT, and ultrasound (US) imaging, have been widely used in the diagnosis of various diseases with the assistance of medical image analysis techniques. For diagnosing brain, vertebra, and oral diseases, CT and MRI are two of the most popular imaging modalities. However, for observing features and estimating diseases from a series, brain, vertebra and oral CT and MRI are challenging. Therefore, this study developed the NIFCM with GA to help identify lesions, segment organs, and help guide surgical processes. Moreover, the proposed method and comparison method, which are traditional FCM, IFCM with manual setting, can be implemented, and the NIFCMGA also examined the Gaussian low-pass filter in the study. In the study, two MRI and two CT images, respectively, brain tumor MRI, vertebra MRI, a tumor vertical view CT in alveolus, and a tumor lateral view CT in alveolus, were examined. The brain tumor MRI is from Karayiannis and Pai (1999). The vertebra MRI and two CT images are sourced from a professional hospital. To verify the performance of the segmentation of the proposed method against other methods, a ground truth image or manually segmented images are taken. In each of the methods, misclassification error was calculated using Eq. (16) with the number of noise pixels, in which the class of pixel differs from that of neighboring pixels. Intuitively, a lower number of noise pixels is a clear indication of a higher quality image. Furthermore, the intuitive judgment from a professional physician, which can be determined by the ratings *excellent*, *good*, *average*, *weak* and *poor,* can also be considered for verifying the performance of segmentation. Intuitive judgment is provided by a professional physician; therefore, the estimated ranking of methods may be more precise, considering that superior methods are better able to assist in the diagnosis of disease.

5.1 Parameters experiment

The FCM, IFCM, NIFCMGA, models were coded in MATLAB 7.0. First, different m values of weighting exponent on each fuzzy membership (1.5, 2.0, 2.5, and 3.0), using experimental settings from Hung et al. (2011), were tested in the FCM and IFCM, and the parameter of Yager's intuitionistic fuzzy complement was set at $\alpha = 2$ in the IFCM and NIFCM models, as been suggested by Chaira (2011). The parameters of NIFCMGA were determined by GA in this research. Table 3 shows the results of various models with different m values in four images.

In the parameters experiment, some phenomena can be observed as follows: (1) FCM with various m values obtained worse performances than other methods in brain tumor MRI, Vertebra MRI, and two tumor vertical view CT images. (2) IFCM easily results in overfitting in the two CT images. (3) NIFCMGA with $S = 4$ has outperformance in all images, respectively. (4) NIFCMGA with testing parameters robustly obtained images and better performances in our cases. The reason is that NIFCM adopts the neighborhood mechanism to modify the clustering membership, which can effectively provide stable membership values in observing the parameters. (5) Although using NIFCMGA may cost more CPU time than traditional methods, the results of NIFCMGA can evidence that NIFCMGA clustering technology fits more for handling the medical images.

5.2 Experimental results

Figure 2 shows the experiment results of a brain tumor MRI using various clustering methods. In Fig. 2a, the original brain MRI is poorly illuminated. The brain tumor MRI is used to evaluate the segmented images, as the tumor appears very bright and is well separated from surrounding tissue. The red cycle region indicates a brain tumor. Observing the results of three clustering methods, some phenomena can be observed: (1) Fig. 2b and c shows that the FCM and IFCM can clearly index the tumor, but the two methods have more noise effects; (2) in Fig. 2d, the NIFCMGA clustering technology can also clearly index the tumor, and reduce noise effects. (3) A Gaussian low-pass filter was used to reduce the noise in the image presented in Fig. 2e, f. Unfortunately, this process also removed details required to render the shape of the brain tumor and the texture of the brain, as shown in Fig. 2e and f.

Table 4 shows that the NIFCMGA obtains superior performance whether it is estimated by a misclassification error index or by intuitive judgment. The NIFCMGA has a lower misclassification error. Moreover, in an intuitive judgment, the NIFCMGA also is judged as being *Good* by professional physicians.

Figure 3 shows the experiment results of a b vertebra MRI using various clustering methods. In Fig. 3a, the original vertebra MRI is very ambiguous. Figure 3b and c shows that the FCM and IFCM cannot effectively reduce noise effects; otherwise in Fig. 3d, the NIFCMGA clustering technology can also provide clear and high quality image, and reduce noise effects. Using Gaussian low-pass filter cannot clearly show the texture of vertebra MRI in Fig. 3e, f. Table 4 shows that the NIFCMGA obtains superior performance whether it is estimated by a misclassification error index or by intuitive judgment. The NIFCMGA is judged as being *Excellent* by professional physicians.

Table 3 Testing error (E) of various models with different m values

Method	Parameters	Error (E) $\times 10^{-5}$	No. of noise pixel/CPU time (Min)
Brain tumor MRI (Cluster = 4)			
FCM	$m = 1.5$	407.24	72/0.1341
	$m = 2.0$	333.71	59/0.0956
	$m = 2.5$	435.52	77/0.1518
	$m = 3.0$	373.30	66/0.1049
IFCM with $\alpha = 2$	m=1.5	333.71	59/0.1641
	$m = 2.0$	333.71	59/0.1109
	$m = 2.5$	339.37	60/0.2773
	$m = 3.0$	378.96	67/0.1419
NIFCM GA	$S = 4$, $m = 2.0008$, $\alpha = 2.9048$	45.24	8/17.2012
Gaussian low-pass filter + NIFCMGA		0	0/17.5197
Vertebra MRI (Cluster = 4)			
FCM	$m = 1.5$	1,170	3066/0.2394
	$m = 2.0$	1,140	2,993/0.0714
	$m = 2.5$	1,140	2,993/0.3513
	$m = 3.0$	1,140	2,993/0.1153
IFCM with $\alpha = 2$	$m = 1.5$	1,550	4,056/0.1770
	$m = 2.0$	1,100	2887/0.0382
	$m = 2.5$	1,100	2887/0.1050
	$m = 3.0$	1,140	2993/0.0685
NIFCMGA	$S = 4$, $m = 2.2571$, $\alpha = 1.0073$	70.19	187/21.3520
Gaussian low-pass filter + NIFCMGA		0	0/21.5410
A tumor vertical view CT (Cluster = 5)			
FCM	$m = 1.5$	19.455	51/0.8904
	$m = 2.0$	26.321	69/0.4700
	$m = 2.5$	20.981	55/0.0886
	$m = 3.0$	24.796	65/0.9555
IFCM with $\alpha = 2$	$m = 1.5$	16.022	42/3.4211
	$m = 2.0$	13.733	36/ 3.9219
	$m = 2.5$	12.970	34/ 2.4831
	$m = 3.0$	38.528	101/ 1.4732
NIFCM GA	$S = 4$, $m = 1.0426$, $\alpha = 1.6936$	4.5776	12/15.3294
Gaussian low-pass filter + NIFCMGA		0	0/16.2598
A tumor lateral view CT (Cluster=5)			
FCM	$m = 1.5$	780	2034/0.7143
	$m = 2.0$	780	2,034/0.2971
	$m = 2.5$	780	2,034/0.2734
	$m = 3.0$	770	2,025/ 0.8161
IFCM with $\alpha = 2$	$m = 1.5$	1190	3113/4.6320
	$m = 2.0$	1,190	3113/ 3.9177
	$m = 2.5$	—	—
	$m = 3.0$	—	—
NIFCMGA	$S = 4$, $m = 2.8851$, $\alpha = 1.7809$	72.861	191/13.2734
Gaussian low-pass filter + NIFCMGA		0	0/12.9299

— Overfitting (image cannot clearly be recognized by a professional physician)

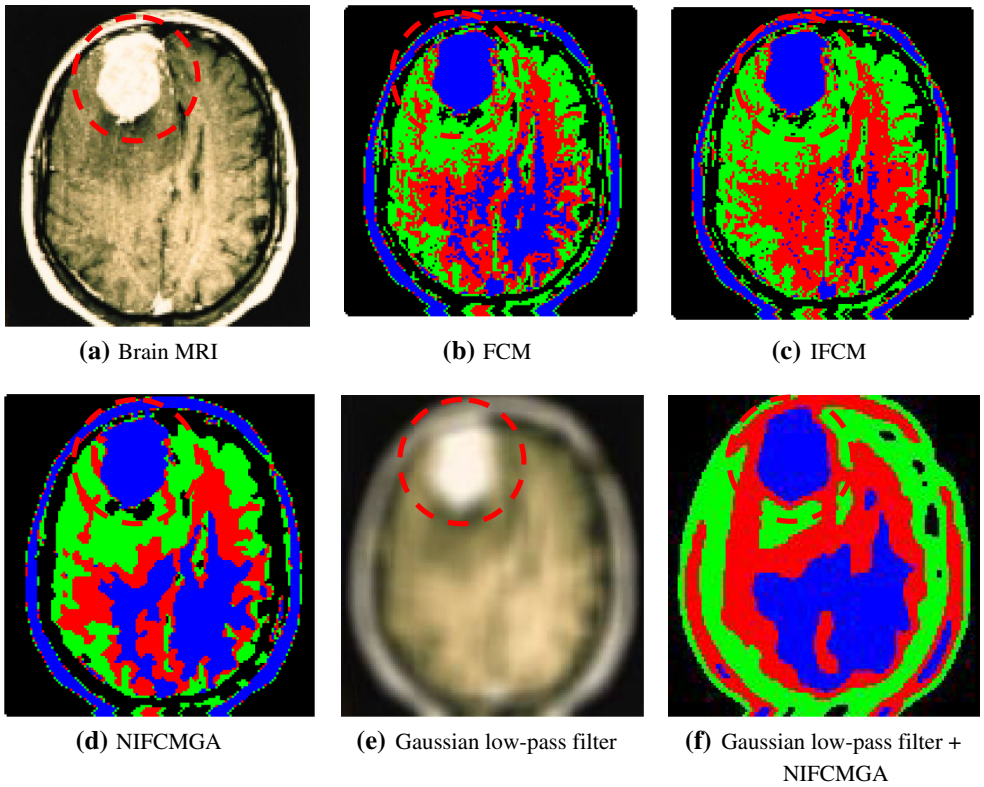

(a) Brain MRI **(b)** FCM **(c)** IFCM

(d) NIFCMGA **(e)** Gaussian low-pass filter **(f)** Gaussian low-pass filter + NIFCMGA

Fig. 2 Experimental results of brain tumor MRI with various clustering methods

Figures 4 and 5 show the results of vertical view of tumor using CT as well as lateral view in the alveolus with various clustering methods. CT image quality is dependent upon balancing these characteristics and parameters to produce the best possible image for the anatomical region being scanned. In Fig. 4a, the vertical view CT is a higher quality image. An overview of Fig. 4 shows that the three methods (Fig. 4b–d) can clearly index the tumor, for the tumor region has a bright background. Notably, traditional FCM may not obtain a clear image from a visual viewpoint. In Fig. 5a, the tumor lateral view CT does not clearly present an image in the tumor region. In Fig. 5b–d, all methods can be shown to clearly index the tumor. The tumor region is brighter than the neighboring regions. Figures 4d, e and 5d, e show the results of Gaussian low-pass filter in the two CT image. In CT image has higher quality image. However, the shape of tumor region also cannot be clearly displayed. Table 4 also shows that the NIFCMGA elicits superior performance in the two CT images.

The NIFCMGA can significantly obtain performance which number of noise pixel can be reduced in all examples. This can evidence the proposed concept of *neighborhood* which can certainly reduce noise effects and provide very clear medical image for professional physician. An overview of the experimental results reveals some phenomena: (1) The NIFCMGA can elicit better performance in MRI and CT images; (2) the proposed concept of *neighborhood* can clearly reduce noise effects and improve IFCM; and (3) although the mechanism of *neighborhood* and GA spend more CPU time, the NIFCMGA can effectively reduce noise pixels in medicine images. (4) The Gaussian low-pass filter can reduce the noise, but the shape and texture cannot clearly display in all image especially diseased region. (5) NIFCMGA provided better performance when the quality of images was poor.

Figure 6 presents histograms of the intensity image in four examples. Outlier regions can be observed from the histogram of an image, indicating the regions with the greatest difference in intensity. For example, the lower intensity regions (the 2 and 3 clusters) are outlier regions in Fig. 6a. The NIFCMGA clustering technique is able to cluster similarity intensities from Fig. 6b, d, f, and h.

6 Conclusions

Numerous studies have focused on fuzzy segmentation methods in medical imaging. This study developed a novel NIFCMGA and applied it to medical imaging. The results indicate that the NIFCMGA model offers a promising alternative for medical image segmentation. The superior performance of the NIFCMGA can be attributed to two factors.

Table 4 A comparison of the misclassification error and intuitive judgment in brain tumor MRI and intuitive judgment in two CT images using various methods

Method	Parameters	Error (E) $\times 10^{-5}$	No. of noise pixel/CPU time (min)	Intuitive judgment[a]
Brain tumor MRI (Cluster = 4)				
FCM	$m = 2.0$	333.71	59/0.0956	Weak
IFCM	m=2.0, $\alpha = 2.0$	333.71	59/0.1109	Weak
NIFCMGA	$S = 4$, $m = 2.0008$, $\alpha = 2.9048$	70.19	187/21.3520	Good
Gaussian low-pass filter + NIFCMGA		0	0/17.5197	Weak
Vertebra MRI (Cluster = 4)				
FCM	$m = 2.0$	1,140	2,993/0.0714	Weak
IFCM	m=2.0, $\alpha = 2.0$	1,100	2,887/0.0382	Average
NIFCMGA	$S = 4$, $m = 2.2571$, $\alpha = 1.0073$	70.19	187/21.3520	Excellent
Gaussian low-pass filter + NIFCMGA		0	0/21.5410	Weak
A tumor vertical view CT (Cluster = 5)				
FCM	$m = 1.5$	19.455	51/0.8904	Weak
IFCM	$m = 2.5$, $\alpha = 2.0$	12.970	34/ 2.4831	Average
NIFCMGA	$S = 4$, $m = 1.0426$, $\alpha = 1.6936$	4.5776	12/15.3294	Excellent
Gaussian low-pass filter + NIFCMGA		0	0/16.2598	Weak
A tumor lateral view CT (Cluster = 5)				
FCM	$m = 3.0$	770	2,025/ 0.8161	Good
IFCM	$m = 2.0$, $\alpha = 2.0$	1,190	3113/ 3.9177	Weak
NIFCM	$S = 4$, $m = 2.8851$, $\alpha = 1.7809$	72.861	191/13.2734	Excellent
Gaussian low-pass filter + NIFCMGA		0	0/12.9299	Good

[a] Intuitive judgment from professional physician

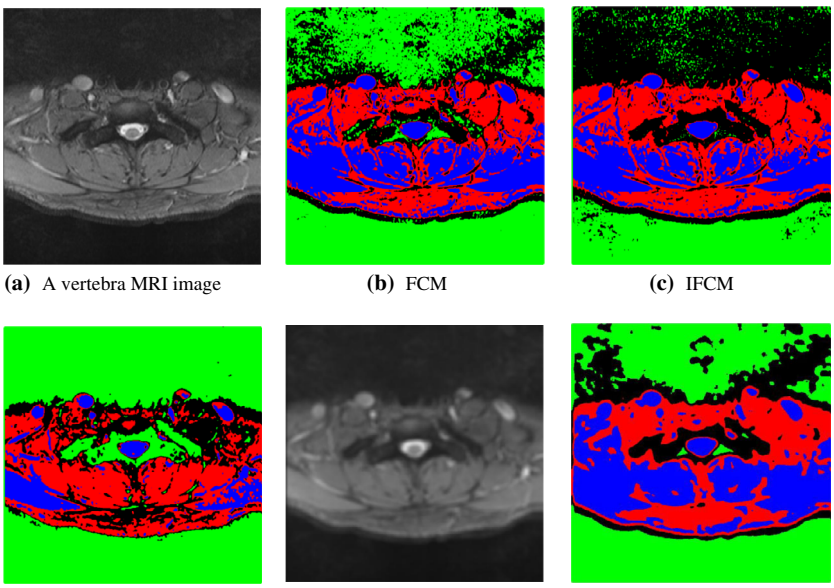

(a) A vertebra MRI image **(b)** FCM **(c)** IFCM

(d) NIFCMGA **(e)** Gaussian low-pass filter **(f)** Gaussian low-pass filter + NIFCMGA

Fig. 3 Experimental results of vertebra MRI example with various clustering methods

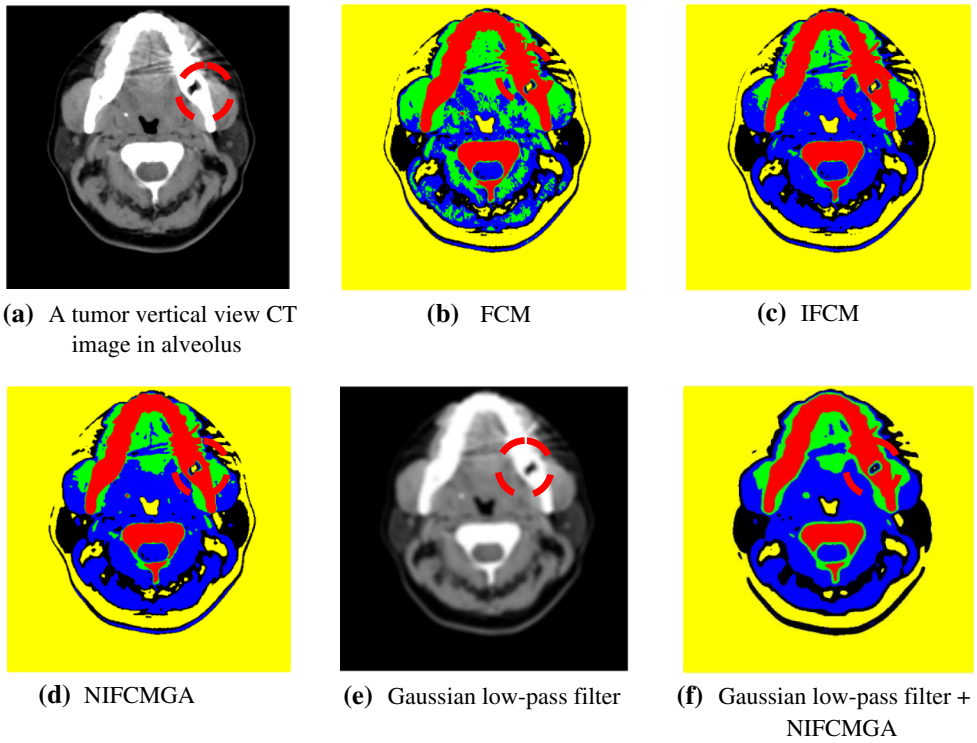

(a) A tumor vertical view CT image in alveolus **(b)** FCM **(c)** IFCM

(d) NIFCMGA **(e)** Gaussian low-pass filter **(f)** Gaussian low-pass filter + NIFCMGA

Fig. 4 Experimental results of tumor vertical view CT in alveolus with various clustering methods

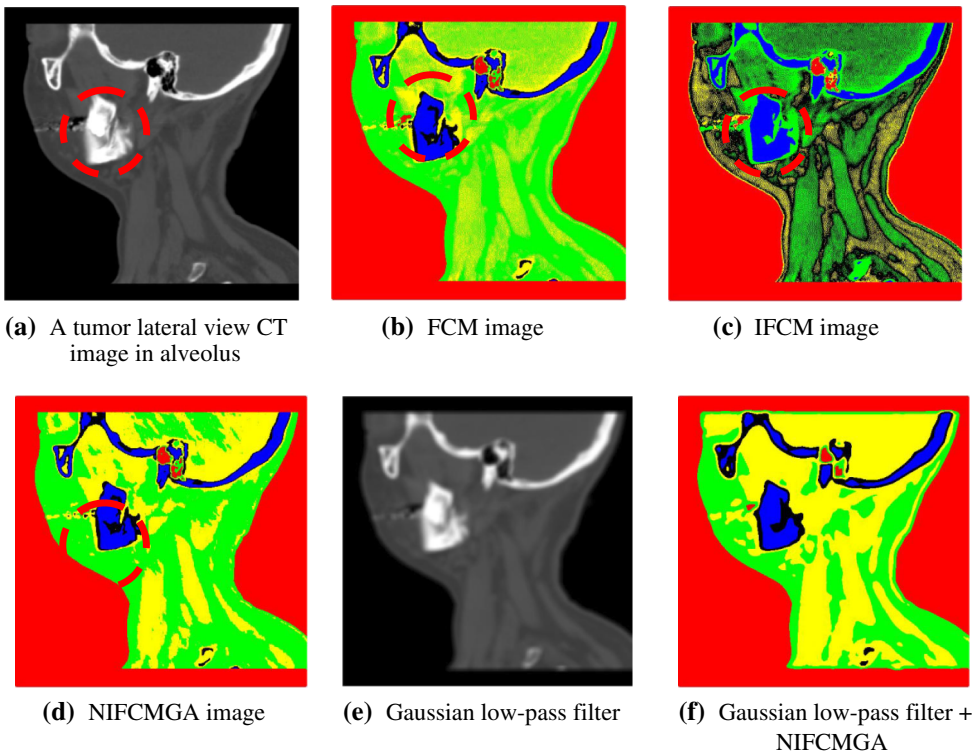

(a) A tumor lateral view CT image in alveolus **(b)** FCM image **(c)** IFCM image

(d) NIFCMGA image **(e)** Gaussian low-pass filter **(f)** Gaussian low-pass filter + NIFCMGA

Fig. 5 Experimental results of tumor lateral view CT in alveolus with various clustering methods

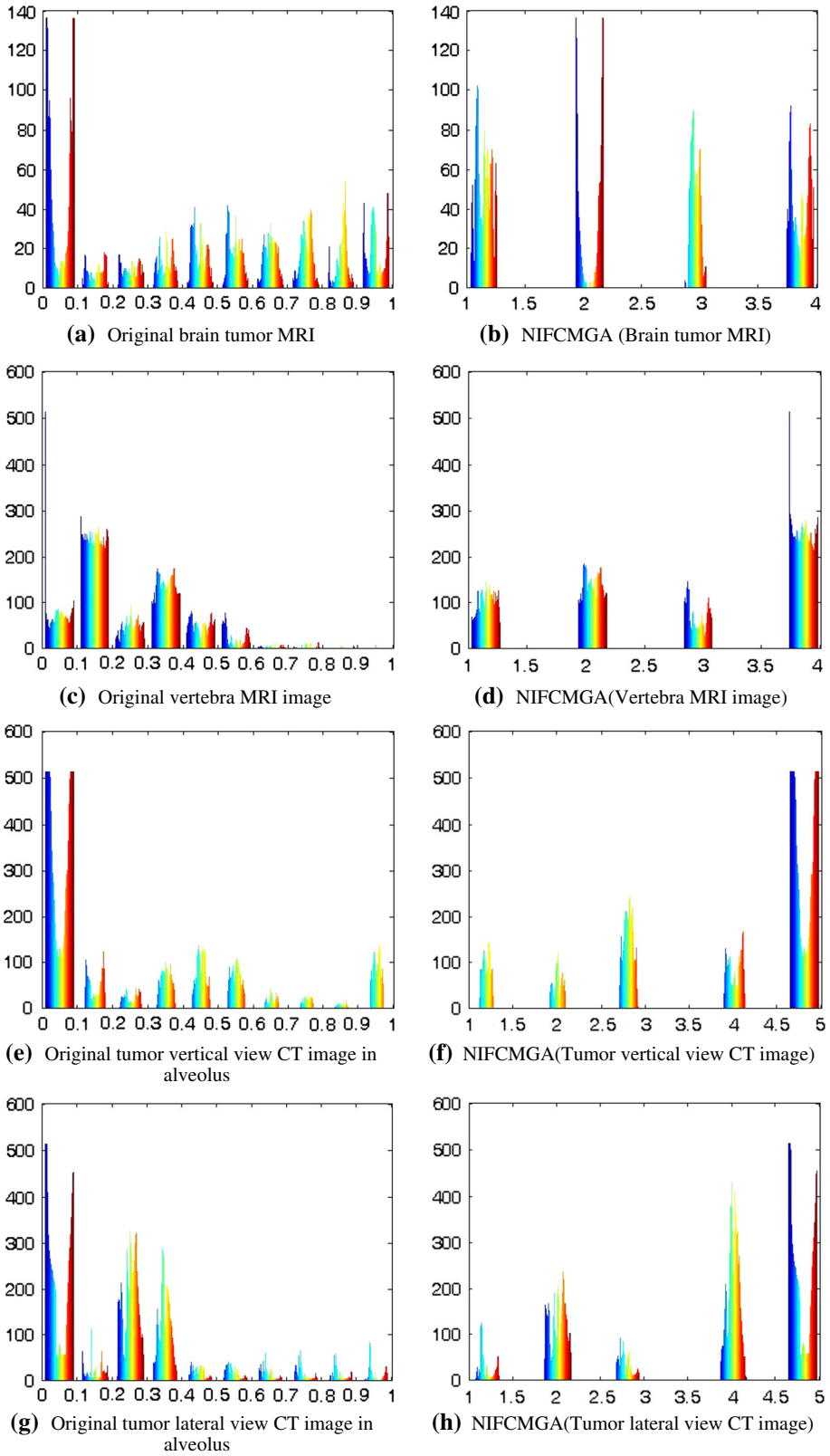

Fig. 6 Comparison of histogram with four examples

First, the concept of neighborhood can reduce noise effects. Second, the GA mechanisms can effectively improve upon the performance of medical image segmentation. The interaction of other types of medical images and the NIFCMGA model may be addressed in future studies, and the other heuristic methods to find global optimal parameters could also be considered for improving the performance, such as immune algorithms, particle swarm optimization, and so on.

Acknowledgments The authors would like to thank National Science Council of the Republic of China for financially supporting this research under Contract No. NSC 102-2410-H-262-008.

References

Atanassov KT (1986) Intuitionistic fuzzy sets. Fuzzy Sets Systems 20:87–96

Atanassov KT (1989) More on intuitionistic fuzzy sets. Fuzzy Sets Systems 33:37–46

Atanassov KT (1999) Intuitionistic fuzzy sets: theory and applications. Physica, Heidelberg

Bezdek JC (1981) Pattern recognition with fuzzy objective function algorithms. Plenum Press, New York

Bezdek JC, Hall LO, Clarke LP (1993) Review of MR image segmentation techniques using pattern recognition. Med Phys 20:1033–1048

Bustince H, Burillo P (1996) Vague sets are intuitionistic fuzzy sets. Fuzzy Sets Systems 79:403–405

Chang PT, Lin KP, Lin CS, Hung KC, Hung LT, Hsu BD (2009) Developing a fuzzy bi-cluster regression to estimate heat tolerance of plants by chlorophyll fluorescence. IEEE Trans Fuzzy Systems 17:485–504

Chaira T (2011) A novel intuitionistic fuzzy C means clustering algorithm and its application to medical images. Appl Soft Comput 11:1711–1717

Chen L, Chen CLP, Lu M (2011) A multiple-kernel fuzzy c-means algorithm for image segmentation. IEEE Trans Systems Man Cybern Part B Cybern 41:1263–1274

Clark MC, Hall LO, Goldgof DB, Clarke LO, Velthuizen RP, Silbiger MS (1994) MRI segmentation using fuzzy clustering techniques. IEEE Eng Med Biol 13:730–742

de Jesús Rubio J, Pacheco J (2009) An stable online clustering fuzzy neural network for nonlinear system identification. Neural Comput Appl 18:633–641

Hruschka ER, Campello RJGB, Freitas AA (2009) A survey of evolutionary algorithms for clustering. IEEE Trans Systems Man Cybern Part C Appl Rev 39:133–155

Fan J, Han M, Wang J (2009) Single point iterative weighted fuzzy C-means clustering algorithm for remote sensing image segmentation. Pattern Recogn 42:2527–2540

He R, Sajja BR, Datta S, Narayana PA (2008) Volume and shape in feature space on adaptive FCM in MRI segmentation. Ann Biomed Eng 36:1580–1593

Holland JH (1975) Adaptation in natural and artificial system. University of Michigan Press, Ann Arbor

Honda K, Ichihashi H (2004) Linear fuzzy clustering techniques with missing values and their application to local principal component analysis. IEEE Trans Fuzzy Systems 12:183–193

Hung CC, Kulkarni S, Kuo BC (2011) A new weighted fuzzy c-means clustering algorithm for remotely sensed image classification. IEEE J Sel Top Signal Process 5:543–553

Hwang C, Rhee F (2007) Uncertain fuzzy clustering: interval type-2 fuzzy approach to c-means. IEEE Trans Fuzzy Systems 15:107–120

Jain AK, Dubes RC (1988) Algorithm for clustering data. Prentice-Hall, New Jersey

Jangjit S (2009) Parameter estimation of three-phase induction motor by using genetic algorithm. J Electr Eng Technol 4:360–364

Ji ZX, Sun QS, Xia DS (2011) A modified possibilistic fuzzy c-means clustering algorithm for bias field estimation and segmentation of brain MR image. Comput Med Imaging Graph 35:383–397

Kannan SR, Ramathilagam S, Sathya A, Pandiyarajan R (2010) Effective fuzzy c-means based kernel function in segmenting medical images. Comput Biol Med 40:575–579

Karayiannis NB, Pai P (1999) Segmentation of magnetic resonance images using fuzzy algorithms for learning vector quantization. IEEE Trans Med Imaging 18:172–180

Kohonen T (1997) Self-organizing maps, 2nd edn. Springer, Berlin

Liu X, Wang L (2007) Computing the maximum similarity bi-clusters of gene expression data. Bioinformatics 23:50–56

Maji P, Pal SK (2008) Maximum class separability for rough-fuzzy c-means based brain MR image segmentation. Lect Notes Comput Sci 5390:114–134

Pedrycz W, Rai P (2008) Collaborative clustering with the use of Fuzzy C-Means and its quantification. Fuzzy Sets Systems 159:2399–2427

Pham DL, Prince JL (1999) Adaptive fuzzy segmentation of magnetic resonance images. IEEE Trans Med Imaging 18:737–752

Shen S, Sandham W, Granat M, Sterr A (2005) MRI fuzzy segmentation of brain tissue using neighborhood attraction with neural-network optimization. IEEE Trans Inf Technol Biomed 9:459–467

Srivastava V, Tripathi BK, Pathak VK (2012) Evolutionary fuzzy clustering and functional modular neural network-based human recognition. Neural Comput Appl 21:1–9

Tao J, Wang N (2007) DNA computing based RNA genetic algorithm with applications in parameter estimation of chemical engineering processes. Comput Chem Eng 31:1602–1618

Tolias YA, Panas SM (1998) A fuzzy vessel tracking algorithm for retinal images based on fuzzy clustering. IEEE Trans Med Imaging 17:263–273

Yang MS (1993) A survey of fuzzy clustering. Math Comput Model 18:1–16

Yasnoff WA, Mui JK, Bacus JW (1977) Error measures for scene segmentation. Pattern Recogn 9:217–231

Zadeh LA (1965) Fuzzy sets. Inf Control 8:338–353

Zhang GP (2000) Neural networks for classification: a survey. IEEE Trans Systems Man Cybern Part C Appl Rev 30:451–462